Transcriptome Analysis of the Liver of Eospalax Fontanierii Under Hypoxia

Zhiqiang Hao
Shaanxi Normal University College of Life Sciences
Lulu Xu
Shaanxi Normal University College of Life Sciences
Jianping He
Shaanxi Normal University College of Life Sciences
Guanglin Li
Shaanxi Normal University College of Life Sciences
Jingang Li (jingang@snnu.edu.cn)
Shaanxi Normal University https://orcid.org/0000-0002-5664-0715

Research

Keywords: Hypoxia adaptation, Eospalax fontanierii, transcriptome

Posted Date: September 15th, 2020

DOI: https://doi.org/10.21203/rs.3.rs-74186/v1

Abstract

Background

Hypoxia can induce cell damage, inflammation, carcinogenesis, and inhibit liver regeneration in non-adapted species. Because of their excellent hypoxia adaptation features, subterranean rodents have been widely studied to clarify the mechanism of hypoxia adaptation. *Eospalax fontanierii*, which is a subterranean rodent found in China, can survive for more than 10 h under 4% O_2 without observable injury, while *Sprague-Dawle* rats can survive for less than 6 h under the same conditions. To explore the potential mechanism of hypoxia adaptation in *E. fontanierii*, we performed RNA-seq analysis of the liver in *E. fontanierii* exposed to different oxygen levels (6.5%, 10.5%, and 21%).

Results

Based on the bioinformatics analysis, 39,439 unigenes were assembled, and 56.78% unigenes were annotated using public databases (Nr, GO, Swiss-Prot, KEGG, and Pfam). In total, 725 differentially expressed genes (DEGs) were identified in the response to hypoxia; six with important functions were validated by qPCR. Those DEGs were mainly involved in processes related to lipid metabolism, steroid catabolism, glycolysis/gluconeogenesis, and the AMPK and PPAR signaling pathway. By analyzing the expression patterns of hub genes related to energy associated metabolism under hypoxia, we found that fatty acid oxidation and gluconeogenesis were increased, while protein synthesis and fatty acid synthesis were decreased.

Conclusions

We characterized the *E. fontanierii* liver transcriptomes and profiled the changes in gene expression in the liver under different oxygen levels. Functional enrichment analysis showed that the main functions (steroid catabolic process, lipid metabolic process, primary bile acid biosynthesis, energy production and amino acid metabolic) of the liver were regulated in response to hypoxia. We identified multiple important DEGs underlying the potential molecular adaptation mechanisms to hypoxia, including genes associated with anti-apoptosis, energy supply, anti-inflammation, and anti-oxidation. Our results provide a comprehensive understanding of the response to hypoxia in *E. fontanierii*, and have potential value for biomedical studies.

Background

Subterranean rodents are highly adaptable to environmental hypoxia [1]. Subterranean rodents such as *Spalax* and *Heterocephalus glaber* (the naked mole-rat, *NMR*) have attracted attention because of their excellent adaptation to hypoxia as well as features of longevity and cancer resistance [2, 3]. Previous studies showed that *hypoxia-inducible factor 1α* (*HIF-1α*) and *erythropoietin* (*Epo*) were upregulated to a higher degree in *Spalax* under normoxia or hypoxia than that in *Rattus*, and contribute substantially to the mechanism underlying adaptive hypoxia tolerance [4]. Several types of globin (neuroglobin, cytoglobin,

and myoglobin) also contribute to the remarkable tolerance of *Spalax* under environmental hypoxia. Transcriptomic studies have shown the involvement of hypoxia-induced genes in *Spalax* in functions including anti-apoptosis, antioxidant defense, DNA repair, cancer, embryonic/sexual development, and epidermal growth factor receptor binding [5–7]. Transcriptomic studies in the NMR showed enrichment of genes in several hypoxia stress-related GO categories, including biological regulation, ion transport, cell-cell signaling, and pathways, such as focal adhesion, the mitogen-activated protein kinase (MAPK) signaling pathway and the glycine, serine and threonine metabolism pathway [8]. Comparative genome analysis in the *NMR* and Damaraland mole-rat showed that the expression of oxygen-carrying globins in the brain contributes to the adaptation to subterranean life [9]. Various studies of hypoxia tolerance mechanisms have been conducted in different subterranean rodents about hypoxia tolerance mechanisms. However, further investigations are required to clarify the mechanisms of hypoxia adaptation in a wider variety of species of subterranean rodents, because the adaptation of subterranean rodents exhibits species specificity [10].

E. fontanierii belongs to the Myospalactinae subfamilies of the family Spalacidea and is a typical subterranean rodent found in China [11–13]. *E. fontanierii* has numerous morphological specializations, such as long claws, small eyes and ears, large keratinized nose, strong zygomatic arch, fused cervical vertebrae, and enlarged olecranon process [14]. In laboratory, *E. fontanierii* can survive more than 10 h under 4% O_2 without visible injury, while *Sprague Dawley rats* (*SD rats*) survive for less than 6 h under the same conditions [15]. Our previous study of *E. fontanierii* skeletal muscle under extreme hypoxia showed that *E. fontanierii* is much more tolerant to hypoxia than the *Sprague Dawley rat*, and significant changes in components of the blood, such as, red blood cell, hemoglobin concentration, hematocrit, mean corpuscular volume, and mean corpuscular hemoglobin, may contribute to hypoxia tolerance [16, 17]. Our subsequent transcriptomic analysis of *E. fontanierii* heart showed that the expression of fibrinogen mRNA was downregulated under hypoxia, which prevented the blood from becoming overly viscous, and protected the heart against thrombosis induced under hypoxia [18]. As hypoxia is often associated with ischemia, inflammation, cancer, and cardiovascular diseases, the hypoxia tolerance trait of *E. fontanierii* has important potential applications in biomedical studies.

The liver, an organ only found in vertebrates, detoxifies various metabolites, synthesizes protein, and produces biochemicals necessary for digestion [19]. Its other roles in metabolism include the regulation of glycogen storage, red blood cells decomposition, and hormones production. The liver also accounts for approximately 20% of resting total body oxygen consumption (details at: https://aneskey.com/liver-anatomy-and-physiology/). Hypoxia induces cell damage, inflammation, carcinogenesis, and inhibits liver regeneration in non-adapted species [20]. Therefore, *E. fontanierii* liver is a useful model for investigations of the hypoxia tolerance.

In this study, we carried out RNA-seq of *E. fontanierii* liver to explore shared or unique molecular mechanisms underlying hypoxia adaptation in subterranean rodents. We analyzed the changes in gene expression following exposure to 21%, 10.5%, and 6.5% oxygen, presenting normoxic, chronic hypoxic and acute hypoxic conditions, respectively, and evaluated the molecular adaptations to hypoxia. Our

results form the basis of further studies of hypoxia adaptation in *E. fontanierii* and have potential biomedical applications.

Results

RNA sequencing and *de novo* transcriptome assembly

In *E. fontanierii*, we performed RNA sequencing of liver organ, and 258.4 million pair-end raw reads were generated. After removal of adapters, primer sequences, and low-quality reads, 239.2 million pair-end clean reads were retained for further analysis. The guanine and cytosine (GC) contents ranged from 49.73% to 52.48%, and Q30 (99.9% base accuracy) scores were ≥85.00% (Table 1). An average of 26.6 million pair-end reads was generated for each sample. All reads were pooled for the *de novo* assembly. There were 39,439 unigenes, in which the N50 length was 2,556 nt, and the median length was 1,412 nt. The lengths of the unigenes ranged from 200~21,949, with the majority distributed in the range of 600~800 nt (Fig. S1A).

In total, 11,667,577 nt (15.6%) of unigene sequences were masked by RepeatMasker, the majority of which were retrotransposons (12.54%) and DNA transposons (0.96%). Alu/B1, B2, and B4 were the three most abundant short interspersed nuclear elements (SINEs). By calculating the best matches with genes/RNAs from nine different rodent species and *Homo sapiens*, homologous genes were identified for a total of 37,789 unigenes (ranges: 30,574~36,539) (blastn, E-value < 1e-5, Table S1).

Gene function annotation and CDS prediction of unigenes

Several databases, such as GO (Fig S2), Nr, Swiss-Prot, Pfam, and KEGG, were searched for functional annotation of unigenes. In total, 56.78% (22,395) unigenes were annotated at least once in the databases searched (Table 2). Furthermore, 16,754 unigenes ≥1,000 nt in length were annotated by the different databases.

A total of 33,003 CDSs were predicted from 30,893 unigenes, of which 1,888 unigenes possessed two or more CDSs. The mean and N50 lengths of CDSs were 814.9 nt and 1,554 nt, respectively. Many short CDSs were in the range of 200-300 nt in length (Fig. S1B). Among the CDSs identified, 58.7% (19,378) were complete. In addition, 46.4% (15,304) and 41.1% (13,561) of the CDSs were annotated by the UniRef90 and Pfam databases (E-value < 1e-5), respectively.

Read-mapping and differentially expressed gene identification

Based on RNA-Seq data, gene expression levels can be quantified by counting reads mapped to transcripts. This process is often influenced by changes in gene length and sequencing depth, alternative splicing, and gene duplication. RSEM enables accurate transcript quantification for species without sequenced genomes. To compare gene expression levels in multiple samples, FPKM values were used to measure the expression levels of unigenes. Overall, expression levels of 87.7% (34,591 of 39,439) of the unigenes were available with FPKM values ≥1 in at least one sample. A majority of the most highly

expressed genes in the live are very important for liver functions (Table S2). For example, apolipoproteins (*APOE*, *APOAI*, *APOA2*, and *APOC1*) are involved in the metabolism of lipoproteins and their uptake in tissues [21]. These genes showed dominant or tissue-specific expression in the liver, with no significant changes in expression under hypoxia, indicating that these proteins facilitate the maintenance of liver function integrity. Hemopexin (*HPX*) prevents the pro-oxidant and pro-inflammatory effects of heme and also promotes its detoxification [22]. Fructose-bisphosphate aldolase B (*ALDOB*) is essential in fructose metabolism [22]. Glutathione S-transferase A1 (*GSTA1*) protects the cells from reactive oxygen species and the products of peroxidation [23]. *HPX*, *ALDOB*, and *GSTA1* under normoxia and hypoxia could protect liver cells from oxidative damage and energy deficiency.

To identify hypoxia-induced DEGs, DESeq2 was used for comparisons between the treatment groups and control groups: 10.5% O_2 vs. 21% O_2; 6.5% O_2 vs. 21% O_2; 6.5% O_2 vs. 10.5% O_2, Fig. S3)[24]. A total of 725 unigenes were considered to be DEGs in response to different hypoxia conditions (Table 3, Table S3). In total, 71.2% (516) of the DEGs were identified in the 6.5% O_2 vs. 10.5% O_2 comparison, while only 4.83% of the DEGs (35 genes) were identified in the 10.5% O_2 and 21% O_2 comparison, suggesting a weak response to chronic hypoxia. Sixty- three upregulated DEGs and 62 downregulated DEGs were found in both the 6.5% vs. 10.5% and 6.5% vs. 21% comparisons. In all the DEG sets, the numbers of downregulated genes exceeded the number of upregulated genes under hypoxia when compared with the numbe. It can be speculated that reduced transcriptional activities may contribute to the tolerance to hypoxia in *E. fontanierii*.

GO enrichment of DEGs

To identify the functions of DEGs induced by hypoxic stress, GO terms were assigned and enriched. The GO term annotations of DEGs were mainly related to metabolic process, biological regulation, response to stimulus, catalytic activity, transporter activity, and molecular function regulator (Fig 1A, Table S4). We found the most enriched GO terms were commonly associated with lipid metabolism (58 genes), heme binding (18 genes), oxygen binding (7 genes), and response to oxygen-containing compounds (48 genes) (Fig. 1B&C, Fig. S4, Table S5). Many GO terms were associated with energy metabolism, such as fatty acid transporter activity, glucose metabolism, threonine metabolism, and acylglycerol metabolism. Along with the metabolism processes under hypoxia, we also identified some GO terms with response functions, such as response to carbohydrate, response to ethanol, response to zinc ion, response to hormone, response to hexose, and response to monosaccarides. We also identified GO terms associated with regulation of these metabolic and response processes, including regulation of hormone levels, negative regulation of gluconeogenesis, regulation of insulin secretion, regulation of hormone secretion, regulation of lipid metabolism, and regulation of peptide transport, of which the former one is statistically significant and the latter five are not significant. These results showed that hypoxic environments alter metabolism in the liver in *E. fontanierii* at numerous molecular levels, and the corresponding responses and regulations accommodate the changes in metabolism to maintain liver cell function.

KEGG enrichment of DEGs

To further explore the interactions among DEGs, the pathways containing DEGs were annotated and enriched using the KEGG database. The DEGs were mainly involved in lipid, amino acid, and carbohydrate metabolism, signal transduction, the digestive and immune system, as well as infectious diseases, endocrine and metabolic diseases (Fig. 2A). As crucial signaling pathways, PPAR and AMPK signaling pathways were found to be enriched among the DEG sets (Fig. 2B, Fig. S5), and both were associated with energy metabolism. In the AMPK signaling pathway, fatty acid oxidation and gluconeogenesis are enhanced under hypoxia stress, while protein synthesis and fatty acid synthesis are repressed (Fig 3A). In the PPAR signaling pathway, fatty acid oxidation, gluconeogenesis, and cholesterol metabolism were enhanced by upregulating the expression levels of related genes under hypoxic stress (Fig. 3B). Other enriched pathways playing key roles in liver functions were also detected, including steroid hormone biosynthesis, cholesterol metabolism, and bile secretion (Fig. 2B). Energy metabolism-associated pathways, such as glycolysis/gluconeogenesis, tyrosine metabolism, and linoleic acid metabolism, and pathways related to the immune system or disease, such as chemical carcinogenesis, antigen-processing and presentations, and metabolism of xenobiotics by cytochrome P450, were also observed (Fig. 2B). Those pathways enriched for DEGs were associated with basic liver functions, which may contribute to the adaptation of the liver under hypoxic stress. Other important pathways and key genes involved in liver cell survival and functional integrity were explored.

FoxO signaling pathway

The growth arrest and DNA damage-inducible (*GADD45beta*) gene, which encodes a component of FoxO signaling pathway (Fig. 4A), is involved in oxidative stress resistance and DNA repair. In this study, we detected 6.86-fold (padj<0.05) and 4.45-fold (padj<0.05) higher expression in acute hypoxia (6.5% O_2) compared with normoxia (21% O_2) and chronic hypoxia (10.5% O_2), respectively. *GADD45beta* could prevent autophagy and apoptosis in rat [25]. Therefore, it can be speculated that upregulated *GADD45beta* expression protects *E. fontanierii* liver cells from apoptosis under acute hypoxia.

Phosphatidylinositol 3,4,5-trisphosphate 3-phosphatase and dual-specificity protein phosphatase PTEN (*Pten*) expression was downregulated by 2.48-fold (padj < 0.05) and 2.71-fold (padj < 0.05) down-regulated expression in acute hypoxia (6.5% O2) compared with normoxia (21% O_2) and chronic hypoxia (10.5% O_2), respectively. PTEN catalyzes dephosphorylation of protein acts as a phosphatase to dephosphorylate phosphatidylinositol 3,4,5-trisphosphate (*PIP3*), which functions as a tumor suppressor by negatively regulating the PI3K-Akt signaling pathway (Fig. 4A). The phosphatase activity of *Pten* may be involved in regulation of the cell cycle, preventing cells from growing, and dividing too rapidly [26]. Furthermore, *Pten* deletion allows nerve regeneration in mice [27]. It can be speculated that *Pten* downregulation inhibits liver cell apoptosis and promotes cell regeneration, thus contributing to the tolerance to acute hypoxia in *E. fontanierii* liver.

BCL2/adenovirus *E1B* 19 kDa protein-interacting protein 3 (*BNIP3*) displayed 3.47-fold (padj < 0.05) and 3.83-fold (padj < 0.05) higher expression under acute hypoxia (6.5% O_2) compared with normoxia (21% O_2) and chronic hypoxia (10.5% O_2), respectively. *BNIP3* is a member of the apoptotic *Bcl-2* family that

induces autophagy, apoptosis, and necrosis [28, 29]. Nuclear *BNIP3* has been shown to acts as a transcriptional repressor to reduce apoptosis-inducing factor expression and increase resistance to apoptosis in *human* malignant gliomas [30]. Thus, combined with the other genes described, *BNIP3* upregulation under acute hypoxia may help to control apoptosis to avoid irreversible liver injury.

Glycolysis /gluconeogenesis pathway

The glycolysis-related genes Glycolysis pathway, hexokinase (*HK*) (4.01 fold-change and padj < 0.05, 2.85 fold-change and padj = 0.15) and glucokinase (*GCK*) (5.05 fold-change and padj < 0.05, 3.19 fold-change and padj < 0.1) were downregulated under acute hypoxia compared with normoxia and chronic hypoxia, respectively, which impedes the conversion of glucose to glucose-6-phosphate (*G6P*) under acute hypoxia (Fig. 4B). *G6PC* encodes glucose-6-phosphatase, which catalyzes the conversion of *G6P* to a phosphate group and free glucose, which is the last step in gluconeogenesis [31]. In the liver of *E. fontanierii*, the upregulated expression of *G6PC* (4.17 fold-change, padj < 0.05) under acute hypoxia compared with chronic hypoxia will facilitate gluconeogenesis (Fig. 4B). These results showed that under hypoxia, glucose consumption in the liver is reduced, while production supply for other tissues, such as the brain, is increased.

Validation of six DEGs

We selected six genes that were found to be upregulated in the liver under hypoxia by RNA-seq for validation by quantitative real-time PCR (qRT-PCR) (Fig. 5A-F). Three of the genes [very long-chain acyl-CoA synthetase (*Slc27a2*), carnitine O-palmitoyltransferase 1 (*Cpt1a*), and cholesterol 7-alpha-monooxygenase (*Cyp7a1*)] were included in PPAR pathway, while the other three genes [Metallothionein (*MT*), C4b-binding protein beta chain (*C4bpb*), and Hyaluronidase-2 (*Hyal2*)] were key genes in liver functions (Fig. 3B). The qRT-PCR results were generally consistent with RNA-seq data, which showed that all of genes were significantly upregulated under acute hypoxia compared with normoxia or chronic hypoxia. In the qRT-PCR results, *MT*, *Cpt1a*, and *Cyp7a1* were significantly upregulated under acute hypoxia compared with normoxia and chronic hypoxia, simultaneously. *Slc27a2*, *C4bpb*, and *Hyal2* were significantly up-regulated in acute hypoxia and chronic hypoxia compared with normoxia. As these genes are highly important in maintaining liver function, we investigated their functions under hypoxic stress.

Very long-chain acyl-CoA synthetase (*Slc27a2*), which converts free long-chain fatty acids into fatty acyl-CoA esters, and plays key role in lipid biosynthesis and fatty acid degradation [32]. Carnitine O-palmitoyltransferase 1 (*Cpt1a*) catalyzes the transfer of the acyl group from CoA to carnitine to form palmitoylcarnitine as the first and rate-limiting step in the carnitine palmitoyltransferase system. The acyl carnitine is then shuttled across the inner mitochondrial membrane by a translocase [33]. *Slc27a2* and *Cpt1a* are crucial for the activation and oxidation of fatty acids. In the *E. fontanierii* liver transcriptome, *Slc27a2* and *Cpt1a* were upregulated by 2.14-fold (padj < 0.05) and 3.19-fold (padj < 0.05) under acute hypoxia compared with normoxia, respectively. The results suggested that the upregulated expression of *Slc27a2* and *Cpt1a* in the liver of *E. fontanierii* under acute hypoxia could increase the local energy supply

through oxidation of fatty acids, especially when the levels of glucose as the energy supply in the liver were decreased.

Cholesterol 7-alpha-monooxygenase (*Cyp7a1*), which plays an important role in cholesterol metabolism, converts cholesterol to 7-alpha-hydroxycholesterol, in the first and rate-limiting step in bile acid synthesis [34]. Our results showed that *Cyp7a1* in the liver was upregulated by 3.29-fold (padj < 0.05) under acute hypoxia compared with normoxia, which could contribute to bile acid biosynthesis and regulation of cholesterol levels.

Metallothionein (*MT*) has been reported to function as a negative regulator of apoptosis [35]. In *E. fontanierii* liver, *MT* contains 61 residues, including 20 cysteine residues. As a cysteine-rich protein, *MT* performs important functions in the control of oxidative stress, by capturing damaging oxidant radicals, such as superoxide, and hydroxyl radicals via the cysteine residues [36]. In our study, *MT* was upregulated by 3.26-fold (padj < 0.05) and 3.22-fold (padj < 0.1) under acute hypoxia compared with normoxia and chronic hypoxia, respectively. These results indicate that *MT* protects *E. fontanierii* liver tissue against the harmful influences of acute hypoxia.

C4b-binding protein beta chain (*C4bpb*), which is the main inhibitor of the classical complement activation pathway, accelerates the decay of C3-convertase and hydrolyzes the C4b complement fragment [37]. It also interacts with anticoagulant protein S, and binds apoptotic and necrotic cells as well as DNA to clean up after injury and limit the inflammatory potential of necrotic cells [38, 39]. In this study, *C4bpb* was upregulated by 2.78-fold (padj < 0.05) under acute hypoxia compared with normoxia. The finding indicated that upregulated *C4bpb* in acute hypoxia plays a role in preventing the inflammation and blood coagulation induced by acute hypoxia. *C4bpb* negatively regulates complement activation, and its upregulated expression may helps to reduce coagulation under hypoxia, which is consistent with previous study in *E. fontanierii* heart tissue [18].

Hyaluronidase-2 (*Hyal2*) is thought to be involved in cell proliferation, migration, and differentiation [40, 41]. Various functions have been described for the gene, such as response to reactive oxygen species, positive regulation of inflammatory response, negative regulation of protein kinase, cellular response to tumor necrosis factor, and homeostatic processes [42]. In our study, *Hyal2* was upregulated by 2.85-fold (padj < 0.05) and 3.04-fold (padj < 0.05) under acute hypoxia compared with normoxia and chronic hypoxia, respectively, suggesting that upregulated *Hyal2* is an important gene in regulating multiple responses to hypoxia.

DEGs with the GO term “response to hypoxia”

Apart from the DEGs validated by qRT-PCR, we identified some DEGs assigned the GO term “response to hypoxia”, which may play key roles in hypoxia adaptation in subterranean animals and have important additional functions. Compared with normoxic conditions, cystathionine beta-synthase (*Cbs*) and heme oxygenase 1 (*Hmox1*) were upregulated by 2.11-fold (padj < 0.05) and 3.29-fold (padj < 0.05) under acute hypoxia, respectively. *Cbs* catalyzes the first step in the trans-sulfuration pathway, from homocysteine to

cystathionine, which is the precursor of cysteine. In mammals, *Cbs* is a highly regulated enzyme, which contains a heme cofactor that functions as a redox sensor [43]. In our study, *Cbs* was assigned to multiple GO terms that may contribute to liver hypoxia tolerance, such as oxygen binding, carbon monoxide binding, cysteine synthase activity, nitrite reductase (NO-forming) activity, selenocystathionine beta-synthase activity, superoxide metabolic process and negative regulation of apoptotic. *Hmox1* catabolizes free heme, produces carbon monoxide (CO), and induces the upregulation of interleukin 10 (*IL-10*) and interleukin 1 receptor antagonist (*IL-1RA*), which form the basis of its anti-inflammatory properties [44]. Certain important GO terms associated with hypoxia adaptation, such as liver regeneration, negative regulation of extrinsic apoptotic signaling pathway via death domain receptors, positive regulation of angiogenesis, erythrocyte homeostasis, regulation of blood pressure and cellular iron ion homeostasis, were assigned to *Hmox1*. Under hypoxia, hypoxia-inducible factor 1-alpha (*HIF-1-alpha*) is often significantly upregulated [45], and is considered to be the master transcriptional regulator of cellular and developmental responses to hypoxia [45, 46]. As a component of the HIF signaling pathway, *HIF-1* could induce upregulation of *Hmox1* expression under acute hypoxia to promote protection of the liver.

Compared with chronic hypoxia, heme oxygenase 2 (*Hmox2*) and eukaryotic translation initiation factor 4E-binding protein (*EIF4EBP1* or *4E-BP1*) were upregulated by 2.02-fold (padj < 0.05) and 3.20-fold (padj < 0.05) under acute hypoxia, respectively. As a modifier in the regulation of hemoglobin metabolism, *Hmox2* has been reported to contribute to high-altitude adaptation in Tibetans [47]. *EIF4EBP1* is a repressor of translation initiation that regulates *eIF4E* activity by preventing its assembly into the *eIF4E* complex [48]. In the AMPK signaling pathway, upregulated *EIF4EBP1* inhibits protein synthesis and reduces cell activity to save energy (Fig. 3A).

Discussion

E. fontanierii has the ability to tolerate very low oxygen concentration, showing adaptation to the hypoxic environment underground. The extent to which genes remodel their transcriptomes under different oxygen concentrations is not clear in *E. fontanierii*. By profiling the transcriptomes in the liver of *E. fontanierii*, we characterized the DEGs in response to different oxygen concentrations. Most DEGs were identified in comparison of the transcriptomes under chronic hypoxia and acute hypoxia, displaying different mechanisms underlying the response to different oxygen concentrations. In comparisons with normoxia, fewer DEGs were identified in response to chronic hypoxia than to acute hypoxia, suggesting only minor changes in the *E. fontanierii* liver transcriptome as the conditions changed to chronic hypoxia from normoxia. This indicates excellent adaptation to chronic hypoxia during the long-term evolution of *E. fontanierii* in subterranean conditions.

Several genes that were upregulated under acute hypoxia compared with normoxia were enriched in the GO term “negative regulation of apoptosis”. This term was not present in the enriched pathways for upregulated DEGs in chronic hypoxia compared with normoxia, which may be due to the lower number of anti-apoptosis genes identified as DEGs under chronic hypoxia. These findings suggest that the anti-

apoptotic ability of liver cells is enhanced to survive in the adversity associated with acute hypoxia. The negative regulation of apoptosis as a response to hypoxia in the liver in *E. fontanierii* identified in this study is shared by another subterranean mole-rat *Spalax*, indicating different subterranean rodents may share a similar strategy for coping with hypoxia [5, 49]. Hypoxia increases the generation of mitochondrial reactive oxygen species [50], which lead to a harmful oxidation effects [51]. The upregulated expression of antioxidant genes (*MT*, *Cbs*) in *E. fontanierii* liver under hypoxia may prevent oxidative damage. *Cbs* serves as a CO-sensitive modulator of H_2S to support bile excretion and has a putative role in bile-dependent detoxification processes [52]. In the enriched pathways “glycine, serine and threonine metabolism” and “cysteine and methionine metabolism”, *Cbs* catalyzes the conversion of homocysteine to cystathionine, which is converted to cysteine by gamma lyase [53]. Cystathionine protects against endoplasmic reticulum stress-induced lipid accumulation, tissue injury, and apoptotic cell death [54]. Cysteine is the rate-limiting factor in the biosynthesis of glutathione, an amino acid that is relatively rare in foods. Glutathione is one of the major endogenous antioxidants produced by cells and participates directly in the neutralization of free radicals and reactive oxygen compounds [55]. This suggests that *Cbs* upregulation plays roles in anti-apoptotic and anti-oxidant processes under conditions of acute hypoxia.

In this study, we characterized the *E. fontanierii* liver transcriptomes and profiled the changes in gene expression in the liver under different oxygen levels. Functional enrichment analysis showed that the main functions (steroid catabolic process, lipid metabolic process, primary bile acid biosynthesis, energy production and amino acid metabolic) of the liver were regulated in response to hypoxia. We identified multiple important DEGs underlying the potential molecular adaptation mechanisms to hypoxia, including genes associated with anti-apoptosis, energy supply, anti-inflammation, and anti-oxidation. Our study helps to understand the complexity of hypoxic adaptation in *E. fontanierii* liver.

Materials And Methods

Sampling and RNA sequencing

Individuals of *E. fontanierii* (male and female, 220-280 g) were captured from agricultural land in Yan’an (N 35°09', E 109°22'), Shaanxi Province, China. The species conservation status is Least Concern (LC), and the population trend is unknown. All animals were captured and treated humanely according to guidelines of the Care and Uses of Laboratory Animals of China, and all the procedures were approved by the Animal Care and Use Committee of Shaanxi Normal University. The animals were housed in cages [475 L × 350 W × 200 H (mm)] maintained at 21 ± 1 °C and fed with carrots. Experiments were performed under the following conditions: 6.5% O_2 (acute hypoxia), 10.5% O_2 (chronic hypoxia), and 21% O_2 (normoxia) with three biological replicates for each condition. In the normoxia group (21% O_2), animals breathed normal air for 1 week. In the chronic hypoxia group, animals were placed in a hypoxia chamber containing 10.5% O_2 for 44 h. In the acute hypoxia group, animals were placed in 6.5% O_2 hypoxia chamber for 4 h. The chamber was ventilated with nitrogen to maintain a constant oxygen concentration, which was monitored using a JRC-1020 thermo-magnetic analyzer. The animals were anesthetized with

an intraperitoneal injection of pentobarbital and sacrificed to collect fresh tissues and frozen into liquid nitrogen immediately. Total RNA was extracted using an RNA Simple Total RNA kit (TaKaRa) according to the instructions. The total RNA integrity was tested through 1% agarose gel electrophoresis. The RNA concentration was verified with a NanoDrop-2000 spectrophotometer (Thermo Fisher, USA). The cDNA library preparation was performed according to the standard protocol for Illumina sample preparation. The mRNA was enriched using magnetic beads with oligo(dT), and then random fragments of mRNA were generated by adding fragmentation buffer. The mRNA was reverse transcribed into the first-strand cDNA using a six-base random primer, and the second-strand cDNA was synthesized by addition of dNTPs, DNA polymerase I, RNase H, and buffer. The cDNA was purified with Ampure XP beads to obtain double-stranded cDNA. After end repair, the products were purified by AMPure XP beads and were amplified by PCR to construct cDNA library. The concentration and insert size of cDNA libraries were evaluated by Qubit2.0 and Agilent 2100, and effective concentration was estimated precisely by qRT-PCR. After complying with the quality control criteria, cDNA libraries were sequenced using the Illumina HiSeq™ 2500 sequencing platform.

Assembly and Annotation

To obtain clean data, raw data containing adapters and primer sequences were removed, and low-quality bases were filtered by cutadapt (version 1.16) [56]. Trinity (version: 2.4) was applied for *de novo* assembly of Bruijn graphs and full-length transcripts (command: Trinity –seqType fq –left reads.fq –right reads_2.fq –CPU 24 –max_memory 256G) [57]. Unigenes were used to represent one or more transcripts in the same cluster. To display its sequence and avoid redundancy, the sequence of the primary mRNA with the highest expression level or the longest length was regarded as the unigene sequence when the whole genomic sequences were unknown. An isoform was first identified as the unigene sequence with the highest expression (>50% total expression value). If this criterion was not satisfied, the isoform with the longest length was considered to be the unigene sequence. The unigenes with at least 10 read in at least two samples were retained by in-house perl script. Software CD-HIT (version 4.8.1) was used to cluster unigene sequences with a sequence identity threshold of 0.9. RepeatMasker (version open-4.0.7) was used to mask the repeat elements in unigene sequences with nhmmscan as engine (version 3.1b1) and *Mus musculus* as the query species [58]. RNA sequences from 10 species used for homology searches were downloaded from NCBI RefSeq (Table S6). BLAST (version: 2.6.0+) searches for unigene sequences were performed against Nr (blastx, E-value<1e-3, command: blastall -p blastx -i input -d nr -e 1e-3 -m 7 -v 20 -b 20 -o output) and Swiss-Prot (blastx, E-value < 1e-10) databases. To annotate the transcriptome, blastx searches against the Nr database were performed for all unigenes (E-value < 1e-3). Functional annotation with gene ontology (GO) terms was conducted using Blast2GO software, which is designed for the high-throughput and automatic functional annotation of DNA or protein sequences based on the gene ontology vocabulary. Blast2GO Command Line (version:1.3.2) (downloaded from http://www.blast2go.com/blast2go-pro/blast2go-command-line) used the BLAST output to map and annotate unigenes (E-value < 1e-6, command: Blast2GO_HOME/blast2go_cli.run -properties cli.prop -loadfasta input.fasta -loadblast blastResult.xml -mapping -annotation -saveb2g -savedat -annex -useobo go-basic.obo) [59]. Unigene sequences were uploaded into KOBAS3.0 to search for functional annotation

in the Kyoto Encylopedia of Genes and Genomes (KEGG) [60]. The predicted peptide sequences of unigenes were searched against Pfam (E-value ≤ 1e-5, command: phmmer -E 1e-5 -cpu 8 -pfamtblout output input.pep Pfam-A.hmm) using HMMER (version: 3.1b2) [61]. TransDecoder (version: 3.0.1) [57, 62] was used to predict potential confident coding sequences (CDS, minimum length: 150 nucleotides) in unigenes and corresponding amino acid sequences based on open reading frame, log-likelihood score, and Pfam alignment information (command 1: TransDecoder.LongOrfs -t input.fasta; command 2: TransDecoder.predict -t input.fasta –retain_pfam_hits) [57].

Expression analysisand DEG identification

We used a script from Trinity toolkit to quantitate transcript abundance (command: TRINITY_HOME/util/align_and_estimate_abundance.pl –transcript Trinity.fasta –seqType –left reads_1.fq –right reads_2.fq –est_method RSEM –aln_method bowtie –trinity_mode –prep_reference –out_dir rsem_outdir). To quantify gene expression levels, we used bowtie (version: 1.2.2) align reads from all samples against transcript set, and RSEM (version: 1.3.0) was used to estimate the expression abundance. DESeq2 from R packages was used to identify DEGs [63]. Unigenes with a false discovery rate (FDR) <0.05 and fold change in expression >2 or <0.5 were considered to be DGEs. We used a perl script (run_DE_analysis.pl) in Trinity2.4 toolkits for DEG detection (Command: TRINITY_HOME/Analysis/Differential Expression/run_DE_analysis.pl –matrix counts.matrix –method DESeq2 –samples_file samples_ described.txt). Functional enrichment analysis for GO terms was performed using the binGO app in Cytoscape3.4 (assesses over- or under-representation: overrepresentation, statistical test: hypergeometric test, multiple testing correction: Benjamini & Hochberg False Discovery Rate (FDR) correction, significance level: 0.05, reference set: Use the whole annotation as the reference set, ontology file: GO_Cellular_Component/Molecular_Function/Biological_Process) [64]. GO annotation was conducted with Blast2GO. KEGG enrichment for DEGs was completed in KOBAS3.0 (hypergeometric test, FDR correction <0.05) [60].

Real-time PCR validation of RNA-seq data

Six DEGs identified in response to hypoxia in the liver were selected to validate the reliability of the RNA-seq data. Gene expression was measured using Step One Real-Time System (ABI) with SYBR Premix ExTaq. Relative gene expression levels were normalized against that of an internal reference gene (β actin) and calculated using the $\triangle\triangle$Ct method. Primers were designed using Primer-BLAST on the NCBI website (Table 4). The expression of each gene was analyzed using three biological replications for each condition. Data were presented as the mean ± standard deviation (SD). SPSS 17.0 statistical software was used for statistical analysis of the data. The the statistical significance of the differences between the groups were evaluated using student's *t*-test. *P*-values of <0.05 were considered to indicate statistical significance.

Accession number

All pair-end read data have been deposited in NCBI Sequence Read Archive (SRA) with BioProject accession: PRJNA497961 (SRA accession: SRR8090385-SRR8090393). This Transcriptome Shotgun Assembly project has been deposited at DDBJ/ENA/GenBank under the accession GHFG00000000. The version described in this paper is the first version, GHFG01000000.

Abbreviations

Q30
99.9% base accuracy
DEGs
Differentially Expressed Genes
Lv6
liver tissue under 6.5% O_2 concentration
Lv10
liver tissue under 10.5% O_2 concentration
Lv21
liver tissue under 21% O_2 concentration
KEGG
Kyoto Encyclopedia of Genes and Genomes
Pfam
Pfam protein domain database
Nr
RefSeq Non-redundant protein sequences
GO
Gene Ontology.
BP
Biological Process
MF
Molecular Function
CC
Cellular Component
FPKM
Fragments Per Kilobase of transcript per Million mapped reads

Declarations

Acknowledgments

The authors would like to thank all the reviewers who participated in the review and MJEditor (www.mjeditor.com) for its linguistic assistance during the preparation of this manuscript.

Funding

The work was supported by grants from the National Natural Science Foundation of China (No.30670360, No.31770333), and Natural Science Basic Research Program of Shaanxi (Program No.2019JM-287, No.2020JM-300)

Author information

Zhiqiang Hao and Lulu Xu contributed equally to this work.

Affiliations

College of Life Science, Shaanxi Normal University, Xi'an, China

Zhiqiang Hao, Lulu Xu, Jianping He, Guanglin Li & Jingang Li

Contributions

Conceived and designed the experiments: JL GL JH. Analyzed the data: ZH LX JH. Validation: LX. Contributed reagents/materials/analysis tools: ZH LX. Wrote the paper: ZH JL.

Corresponding author

Correspondence to Guanglin Li & Jingang Li

Ethics declarations

Ethics approval and consent to participate

All animals were captured and treated humanely according to guidelines of the Care and Uses of Laboratory Animals of China, and all the procedures were approved by the Animal Care and Use Committee of Shaanxi Normal University.

Consent for publication

Not applicable

Competing interests

The authors have declared that no competing interests exist.

References

1. *Life Underground: the Biology of Subterranean Rodents*. 2001. 559–560.
2. Deweerdt S. Comparative biology: Naked ambition. Nature. 2014;509(7502):S60-1.

3. Lagunas-Rangel FA. Cancer-free aging: Insights from Spalax ehrenbergi superspecies. Ageing Res Rev. 2018;47:18–23.
4. Shams I, Avivi A, Nevo E. Hypoxic stress tolerance of the blind subterranean mole rat: expression of erythropoietin and hypoxia-inducible factor 1 alpha. Proc Natl Acad Sci U S A. 2004;101(26):9698–703.
5. Malik A, et al. Transcriptome analysis of the spalax hypoxia survival response includes suppression of apoptosis and tight control of angiogenesis. BMC Genom. 2012;13:615.
6. Schülke S, et al. Living with stress: regulation of antioxidant defense genes in the subterranean, hypoxia-tolerant mole rat, Spalax. Gene. 2012;500(2):199–206.
7. Malik A, et al. Genome maintenance and bioenergetics of the long-lived hypoxia-tolerant and cancer-resistant blind mole rat, Spalax: a cross-species analysis of brain transcriptome. Sci Rep. 2016;6:38624.
8. Xiao B, et al. Transcriptome sequencing of the naked mole rat (Heterocephalus glaber) and identification of hypoxia tolerance genes. Biol Open. 2017;6(12):1904–12.
9. Fang X, et al. Adaptations to a subterranean environment and longevity revealed by the analysis of mole rat genomes. Cell Rep. 2014;8(5):1354–64.
10. Jiang M, et al., *Genome-wide adaptive evolution to underground stresses in subterranean mammals: Hypoxia adaption, immunity promotion, and sensory specialization.* Ecology and Evolution, 2020.
11. Zhou C, Zhou K. The validity of different zokor species and the genus Eospalax inferred from mitochondrial gene sequences. Integr Zool. 2008;3(4):290–8.
12. Yang C, et al. Morphological differences of internal organs in two species of zokor and their significance in classification. Acta Theriologica Sinica. 2012;32(3):259–65.
13. Norris RW, et al. The phylogenetic position of the zokors (Myospalacinae) and comments on the families of muroids (Rodentia). Mol Phylogenet Evol. 2004;31(3):972–8.
14. Su J, et al. Phylogenetic relationships of extant zokors (Myospalacinae) (Rodentia, Spalacidae) inferred from mitochondrial DNA sequences. Mitochondrial DNA. 2014;25(2):135–41.
15. Yan T, Fan W, He J. The effect of hypoxia tolerance on cardiac muscle structure of Gansu zokor(Myospalax cansus). Journal of Shaanxi Normal University. 2012;40(2):62–6.
16. Yuan G, et al. Comparison of Skeletal Muscle Hypoxia Adaptation between Gansu Zokor(Myospalax cansus) and SD Rat. Chinese Journal of Zoology. 2012;47(3):122–8.
17. Jing Y. Blood Composition and its Relationship with Hypoxia Adaptation in Gansu Zokor. Chinese Journal of Zoology. 2006;41(2):112–5.
18. Xu L, et al. Transcriptome sequencing of Eospalax fontanierii to determine hypoxia regulation of cardiac fibrinogen. Mol Biol Rep. 2019;46(6):5671–83.
19. Abdel-Misih SR, Bloomston M. Liver anatomy. Surg Clin North Am. 2010;90(4):643–53.
20. Rosmorduc O, Housset C. Hypoxia: a link between fibrogenesis, angiogenesis, and carcinogenesis in liver disease. Semin Liver Dis. 2010;30(3):258–70.

21. Ramasamy I. Recent advances in physiological lipoprotein metabolism. Clin Chem Lab Med. 2014;52(12):1695–727.
22. Mehta NU, Reddy ST. Role of hemoglobin/heme scavenger protein hemopexin in atherosclerosis and inflammatory diseases. Curr Opin Lipidol. 2015;26(5):384–7.
23. Liang FQ, et al. Enhanced expression of glutathione-S-transferase A1-1 protects against oxidative stress in human retinal pigment epithelial cells. Exp Eye Res. 2005;80(1):113–9.
24. Anders S, Huber W. Differential expression analysis for sequence count data. Genome Biol. 2010;11(10):R106.
25. He G, et al. Gadd45b prevents autophagy and apoptosis against rat cerebral neuron oxygen-glucose deprivation/reperfusion injury. Apoptosis. 2016;21(4):390–403.
26. Chu EC, Tarnawski AS. *PTEN regulatory functions in tumor suppression and cell biology*. Med Sci Monit, 2004. 10(10): p. Ra235-41.
27. Liu K, et al. PTEN deletion enhances the regenerative ability of adult corticospinal neurons. Nat Neurosci. 2010;13(9):1075–81.
28. Burton TR, Gibson SB. The role of Bcl-2 family member BNIP3 in cell death and disease: NIPping at the heels of cell death. Cell Death Differ. 2009;16(4):515–23.
29. Ghavami S, et al. A8/A9 induces autophagy and apoptosis via ROS-mediated cross-talk between mitochondria and lysosomes that involves BNIP3. Cell Res. 2010;*S*100(3):314–31., ,. **20**.
30. Burton TR, Eisenstat DD, Gibson SB. BNIP3 (Bcl-2 19 kDa interacting protein) acts as transcriptional repressor of apoptosis-inducing factor expression preventing cell death in human malignant gliomas. J Neurosci. 2009;29(13):4189–99.
31. Ghosh A, et al. The catalytic center of glucose-6-phosphatase. HIS176 is the nucleophile forming the phosphohistidine-enzyme intermediate during catalysis. J Biol Chem. 2002;277(36):32837–42.
32. Mihalik SJ, et al. Participation of two members of the very long-chain acyl-CoA synthetase family in bile acid synthesis and recycling. J Biol Chem. 2002;277(27):24771–9.
33. Jogl G, Hsiao YS, Tong L. Structure and function of carnitine acyltransferases. Ann N Y Acad Sci. 2004;1033:17–29.
34. Chiang JY. Bile acids: regulation of synthesis. J Lipid Res. 2009;50(10):1955–66.
35. Levadoux-Martin M, et al. Influence of metallothionein-1 localization on its function. Biochem J. 2001;355(Pt 2):473–9.
36. Kumari MV, Hiramatsu M, Ebadi M. Free radical scavenging actions of metallothionein isoforms I and II. Free Radic Res. 1998;29(2):93–101.
37. Hillarp A, et al. The human C4b-binding protein beta-chain gene. J Biol Chem. 1993;268(20):15017–23.
38. Merle NS, et al. Complement System Part II: Role in Immunity. Front Immunol. 2015;6:257.
39. Trouw LA, et al. C4b-binding protein binds to necrotic cells and DNA, limiting DNA release and inhibiting complement activation. J Exp Med. 2005;201(12):1937–48.

40. Triggs-Raine B, et al. Mutations in HYAL1, a member of a tandemly distributed multigene family encoding disparate hyaluronidase activities, cause a newly described lysosomal disorder, mucopolysaccharidosis IX. Proc Natl Acad Sci U S A. 1999;96(11):6296–300.
41. Marei WF, Salavati M, Fouladi-Nashta AA. Critical role of hyaluronidase-2 during preimplantation embryo development. Mol Hum Reprod. 2013;19(9):590–9.
42. Monzon ME, et al. Reactive oxygen species and hyaluronidase 2 regulate airway epithelial hyaluronan fragmentation. J Biol Chem. 2010;285(34):26126–34.
43. Kabil O, Zhou Y, Banerjee R. Human cystathionine beta-synthase is a target for sumoylation. Biochemistry. 2006;45(45):13528–36.
44. Ozono R. New biotechnological methods to reduce oxidative stress in the cardiovascular system: focusing on the Bach1/heme oxygenase-1 pathway. Curr Pharm Biotechnol. 2006;7(2):87–93.
45. Minet E, et al. HIF1A gene transcription is dependent on a core promoter sequence encompassing activating and inhibiting sequences located upstream from the transcription initiation site and cis elements located within the 5'UTR. Biochem Biophys Res Commun. 1999;261(2):534–40.
46. Iyer NV, et al. Cellular and developmental control of O2 homeostasis by hypoxia-inducible factor 1 alpha. Genes Dev. 1998;12(2):149–62.
47. Yang D, et al. HMOX2 Functions as a Modifier Gene for High-Altitude Adaptation in Tibetans. Hum Mutat. 2016;37(2):216–23.
48. Yanagiya A, et al. Translational homeostasis via the mRNA cap-binding protein, eIF4E. Mol Cell. 2012;46(6):847–58.
49. Schmidt H, et al. Hypoxia tolerance, longevity and cancer-resistance in the mole rat Spalax - a liver transcriptomics approach. Sci Rep. 2017;7(1):14348.
50. Chandel NS, et al. Reactive oxygen species generated at mitochondrial complex III stabilize hypoxia-inducible factor-1alpha during hypoxia: a mechanism of O2 sensing. J Biol Chem. 2000;275(33):25130–8.
51. Coppolino G, et al., *Oxidative stress and kidney function: a brief update.* Curr Pharm Des, 2019.
52. Shintani T, et al. Cystathionine beta-synthase as a carbon monoxide-sensitive regulator of bile excretion. Hepatology. 2009;49(1):141–50.
53. Nozaki T, et al. Characterization of transsulfuration and cysteine biosynthetic pathways in the protozoan hemoflagellate, Trypanosoma cruzi. Isolation and molecular characterization of cystathionine beta-synthase and serine acetyltransferase from Trypanosoma. J Biol Chem. 2001;276(9):6516–23.
54. Maclean KN, et al. Cystathionine protects against endoplasmic reticulum stress-induced lipid accumulation, tissue injury, and apoptotic cell death. J Biol Chem. 2012;287(38):31994–2005.
55. Dringen R. Metabolism and functions of glutathione in brain. Prog Neurobiol. 2000;62(6):649–71.
56. Martin M, *Martin M.Cut adapt removes adapter sequences from high-throughput sequencing reads, EMBnet. EMBnet 17:10–12.* Embnet Journal, 2011. **17**(1).

57. Haas BJ, et al. De novo transcript sequence reconstruction from RNA-seq using the Trinity platform for reference generation and analysis. Nat Protoc. 2013;8(8):1494–512.
58. Tarailo-Graovac M, Chen N. *Using RepeatMasker to identify repetitive elements in genomic sequences*. Curr Protoc Bioinformatics, 2009. Chapter 4: p. Unit 4.10.
59. Conesa A, et al. Blast2GO: a universal tool for annotation, visualization and analysis in functional genomics research. Bioinformatics. 2005;21(18):3674–6.
60. Wu J, et al., *KOBAS server: a web-based platform for automated annotation and pathway identification*. Nucleic Acids Res, 2006. **34**(Web Server issue): p. W720-4.
61. Mistry J, et al. Challenges in homology search: HMMER3 and convergent evolution of coiled-coil regions. Nucleic Acids Res. 2013;41(12):e121.
62. Punta M, et al. The Pfam protein families database. Nucleic Acids Res. 2012;40(Database issue):D290–301.
63. Love MI, Huber W, Anders S. Moderated estimation of fold change and dispersion for RNA-seq data with DESeq2. Genome Biol. 2014;15(12):550.
64. Maere S, Heymans K, Kuiper M. BiNGO: a Cytoscape plugin to assess overrepresentation of gene ontology categories in biological networks. Bioinformatics. 2005;21(16):3448–9.

Tables

Table 1 Mapping statistics of clean reads with assembled unigenes

Samples[a]	Clean Reads	Clean Reads Ratio (%)	G+C (%)	≥Q30 (%)	Mapped Reads	Mapped Ratio (%)[b]
Normoxia (21% O_2)	27,854,142	93.94	51.32	85.00	16,837,469	60.45
26,718,742	93.29	52.06	85.10	16,047,727	60.06	
29,040,231	92.45	51.75	85.00	17,804,759	61.31	
Chronic hypoxia (10.5% O_2)	27,103,408	86.76	52.48	85.10	15,537,620	57.33
27,384,840	81.35	52.00	85.10	16,516,472	60.31	
24,116,984	99.75	50.47	92.90	16,003,380	66.36	
Acute hypoxia (6.5% O_2)	23,280,246	90.95	52.19	85.00	13,880,001	59.62
25,090,462	99.46	50.65	93.30	14,717,266	58.66	
28,633,359	99.46	49.73	93.30	17,195,811	60.06	

[a] 21% O_2, 10.5% O_2, and 6.5% O_2 include three biological replicates of *E. fontanierii* for the three oxygen concentrations; [b] the mapped ratio represents the ratio of mapped reads to clean reads

Table 2. Statistical analysis of unigene annotated by each database

Database	Number of annotated unigenes (Length ≥ 1000)	Number of annotated unigenes	Percentage of annotated unigenes
GO	12,497	14839	31.69
KEGG	11,757	15,622	29.81
Pfam	11,396	12,994	28.90
Swiss-Prot	129,15	15,073	32.75
Nr	15,652	20128	39.69
Total	16745	22,395	56.78

Table 3. DEG numbers

DEG sets (%)	All DEGs	Upregulated	Downregulated
6.5 versus 21	308	134	174
6.5 versus 10.5	516	235	281
10.5 verse 21	35	6	29

Table 4. Primer sequences designed for validation of DEGs

Gene ID	primers	primer sequence（5'-3'）	Tm
MT	Forward	GAGGTGCATCGGCACTCTTT	60℃
	Reverse	CTTGGCGACTCTTTAGCGAC	
Cpt1a	Forward	TGAGTGGCGTCCTGTTCG	60℃
	Reverse	CAGATTCGGGTGCTACGG	
Slc27a2	Forward	GTGCTACTATGGCTTTGCGG	60℃
	Reverse	GTCATTCGGTTTCTGTGGCG	
C4bpb	Forward	CCGGGCCTGTGAATGTAAATG	60℃
	Reverse	TGAATCGGAATCCCAGGAGG	
Hyal2	Forward	CACGCCGACCTCAACTAT	60℃
	Reverse	GCCCAGACTCTACCGACAC	
Cyp7a1	Forward	ACTTTCACCAAAACCCTC	60℃
	Reverse	AACATCACTCGGTAGCAG	
β-ACTIN	Forward	CTAAGGCCAACCGTGAAAAGAT	60℃
	Reverse	GACCAGAGGCATACAGGGACA	

Figures

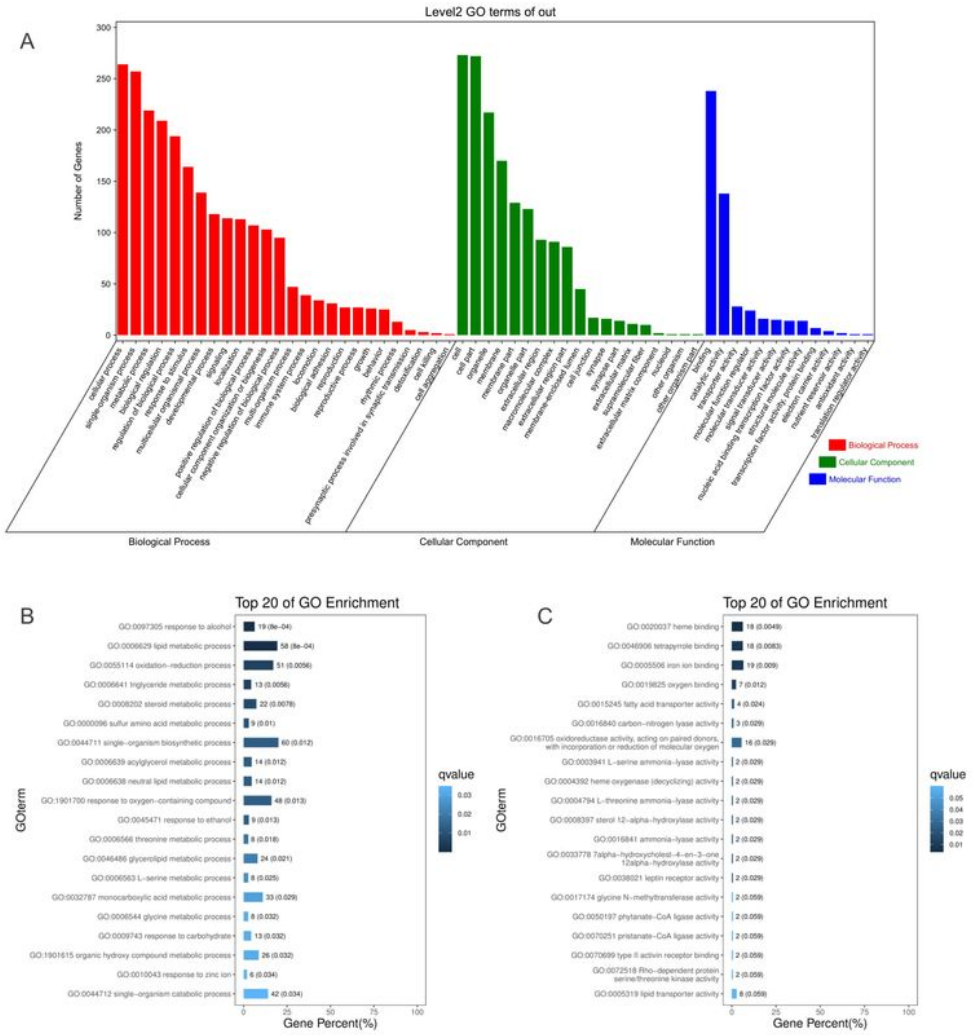

Fig 1. GO annotations of DEGs. (A) GO term classifications in level2 for DEGs, including three parts: Biological Process, Molecular Function, and Cellular Component; (B) Top 20 of GO enrichment on Biological Process for all DEGs; (C) Top 20 of GO enrichment on Molecular Function for all DEGs;

Figure 1

GO annotations of DEGs. (A) GO term classifications (level2) of DEGs, including three catagories: Biological Process, Molecular Function, and Cellular Component; (B) Top 20 of GO enrichment on Biological Process for all DEGs; (C) Top 20 of GO enrichment on Molecular Function for all DEGs;

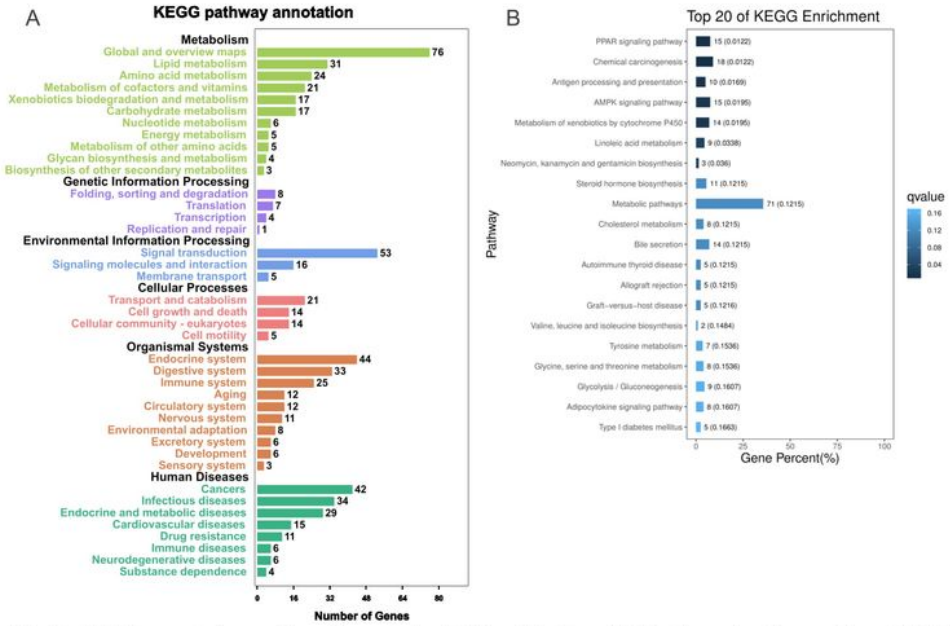

Fig 2. KEGG annotation and enrichment for DEGs. (A) The distribution of pathways for all DEGs annotated by KEGG database. (B) The enriched pathways of all DEGs. The numbers in right space of bars mean the number of DEGs in specific enriched pathway and the numbers in brackets mean the qvalue.

Figure 2

KEGG annotation and enrichment for DEGs. (A) The distribution of pathways for all DEGs annotated in the KEGG database. (B) The enriched pathways of all DEGs. The numbers in right space of bars mean the number of DEGs in specific enriched pathway and the numbers in brackets mean the q-value.

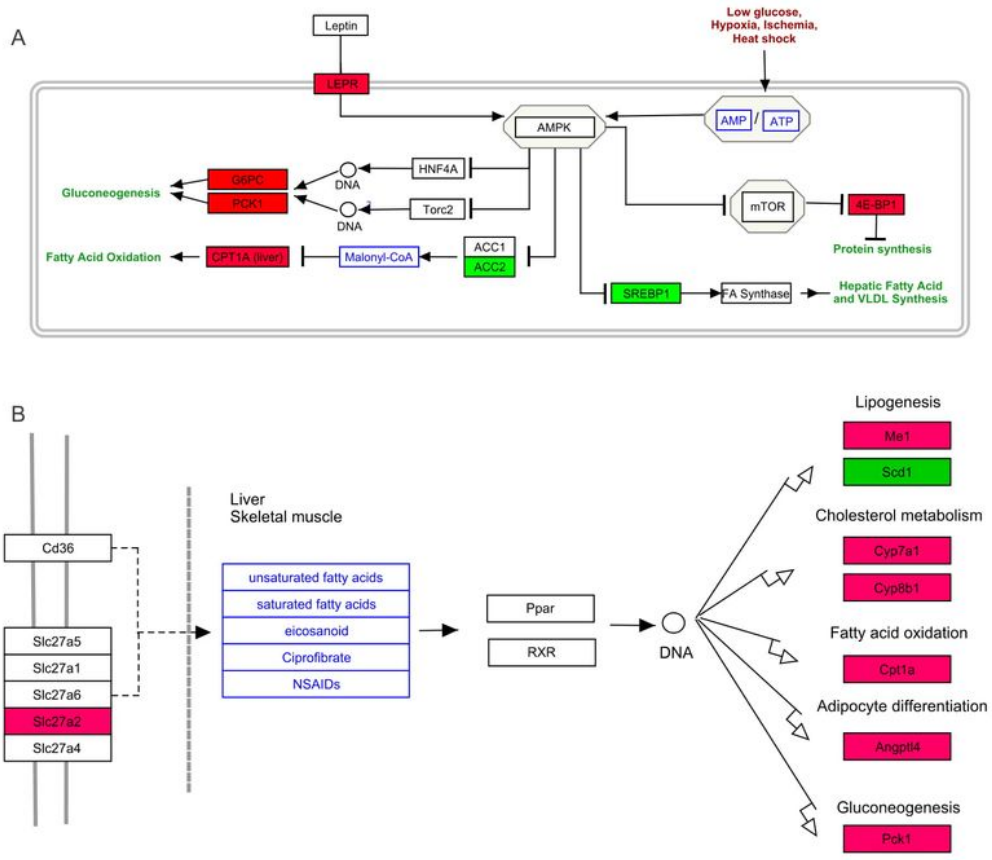

Fig 3. AMPK pathway and PPAR pathway. (A) AMPK pathway; (B) PPAR pathway. Green color means the downregulated DEGs and red color means the upregulated DEGs in hypoxia stress.

Figure 3

AMPK pathway and PPAR pathway. (A) AMPK pathway; (B) PPAR pathway. Green color represents the downregulated DEGs and red color represents the upregulated DEGs in hypoxia stress.

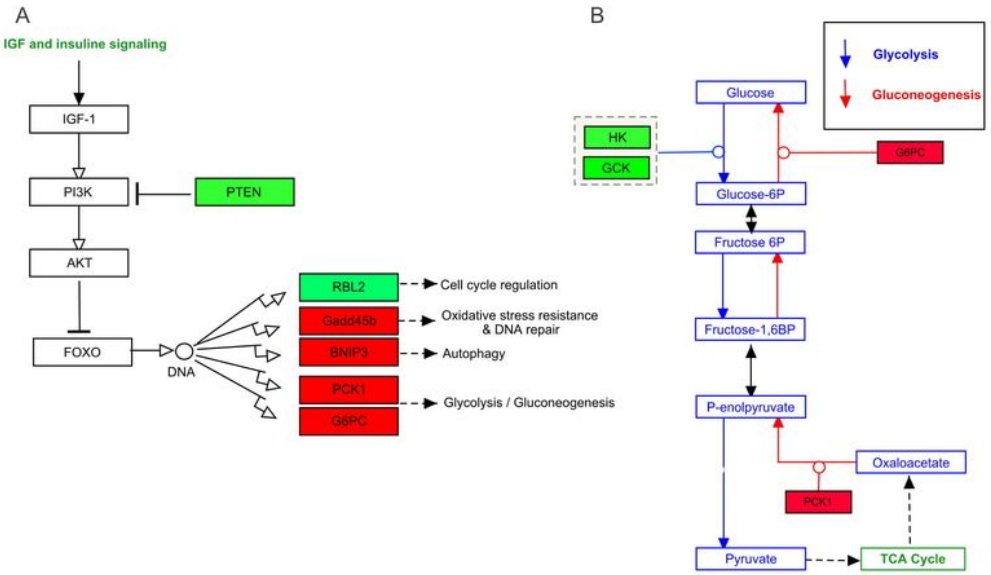

Fig 4. FoxO signaling pathway and PPAR pathway. (A) FoxO signaling pathway; (B) Glycolysis / Gluconeogenesis pathway. Green color means the downregulated DEGs and red color means the upregulated DEGs in hypoxia stress.

Figure 4

FoxO signaling pathway and PPAR pathway. (A) FoxO signaling pathway; (B) Glycolysis/Gluconeogenesis pathway. Green color means the downregulated DEGs and red color means the upregulated DEGs in hypoxia stress, respectively.

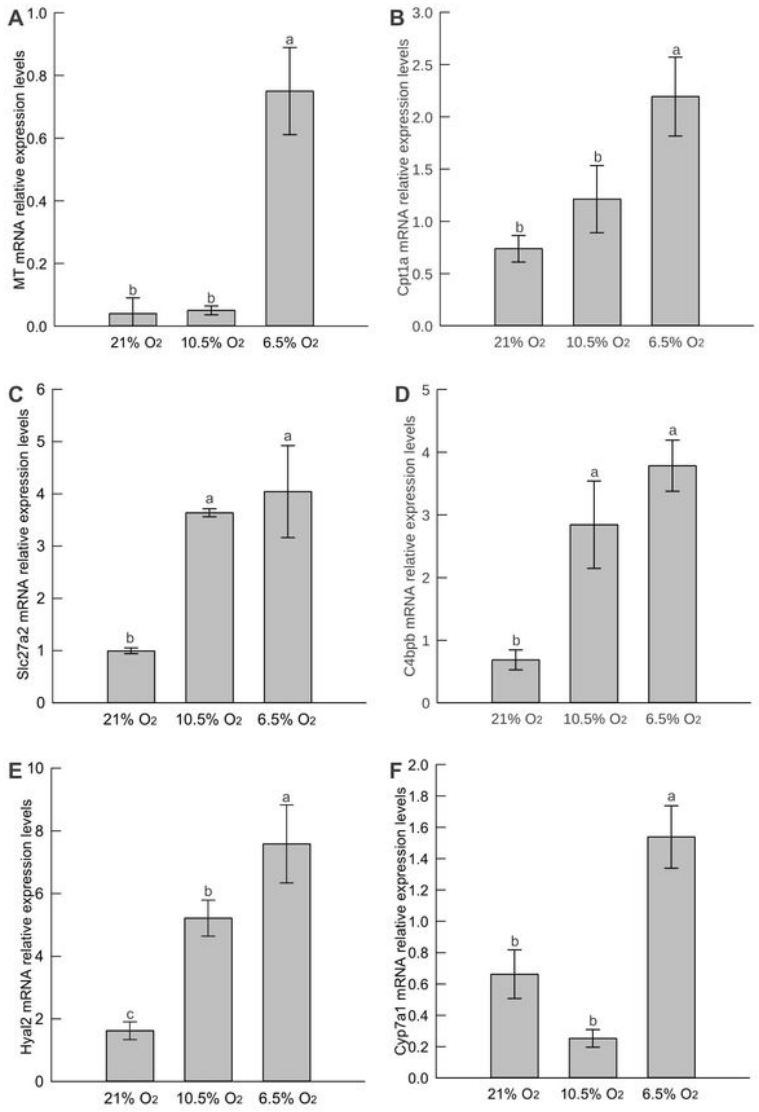

Fig 5. RT-PCR validations for DEGs. (A) MT. (B) Cpt1a. (C) Slc27a2. (D) C4bpb. (E) Hyal2. (F) Cyp7a1. Different alphabetic characters (a, b, and c) above bars represent the gene expression is significantly difference among samples (p-value < 0.05). Same letters mean no significantly difference. All genes used for evaluation were up-regulated under hypoxia (acute or chronic hypoxia) in RNA-Seq experiment.

Figure 5

RT-PCR validations for DEGs. (A) MT. (B) Cpt1a. (C) Slc27a2. (D) C4bpb. (E) Hyal2. (F) Cyp7a1. Different letters (a, b, and c) above bars indicate a significant difference in the gene expression among samples (p-value < 0.05). Same letters indicate no significant difference. All genes evaluated were found to be upregulated under hypoxia (acute or chronic hypoxia) by RNA-seq.

Supplementary Files

This is a list of supplementary files associated with this preprint. Click to download.

- FigS5keggenrichment.pdf
- FigS4GOenrichment.pdf
- FigS3DEGplotv1.pdf
- FigS2geneannotationv3.pdf
- FigS1UnigeneCDSLengthv2.pdf
- TableS5GOout.barGradient.xls
- TableS4GOout.Level2.xls
- TableS3Expressioninfomations.xls
- TableS1S2S6.doc